

University of Illinois at Urbana-Champaign
Summer School on NanoBioPhotonics

Scattering, Absorbing, and Modulating Nanoprobes for Targeted Imaging and Therapy

Stephen A. Boppart, M.D., Ph.D.

*Beckman Institute for Advanced Science and Technology
Departments of Electrical and Computer Engineering,
Bioengineering, Internal Medicine
University of Illinois at Urbana-Champaign*

June 9, 2009

Outline

Lecture 1 (last week)

- Optical Coherence Tomography (OCT)
- Beam Delivery Instruments
- Morphological & Cellular OCT Imaging
- Spectroscopic OCT
- Application to Cancer Imaging



Lecture 2 (today)

- Molecular OCT Imaging
- Contrast Agents for OCT
 - Scattering, Absorbing, Modulating Probes

Combine Optics with Multifunctional Agents

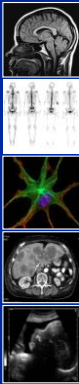
Can leverage the portability and multi-dimensional detection of optics with increasingly powerful and versatile agents for point-of-care detection, imaging, and diagnosis?

<p>Spectroscopic detection Monitoring Drug delivery</p>	<p>Imaging Targeting Therapy</p>
--	---

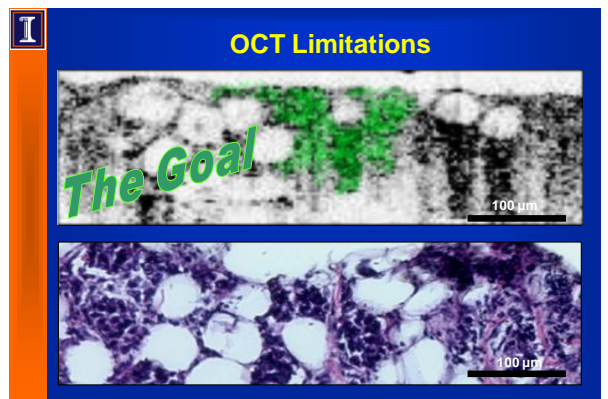
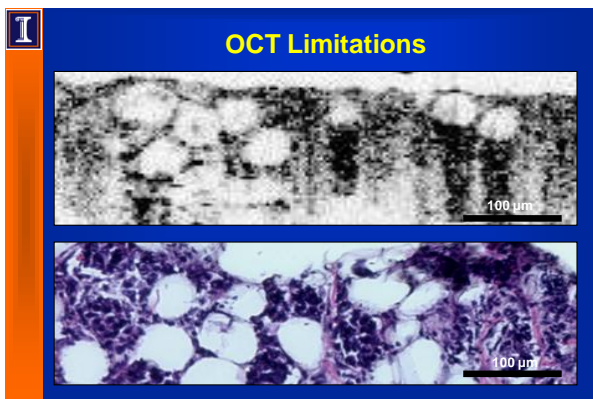
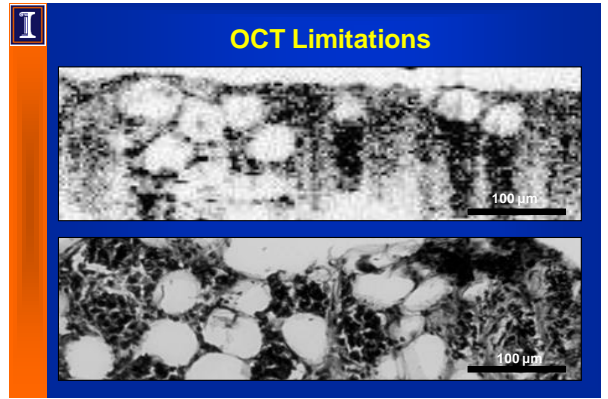
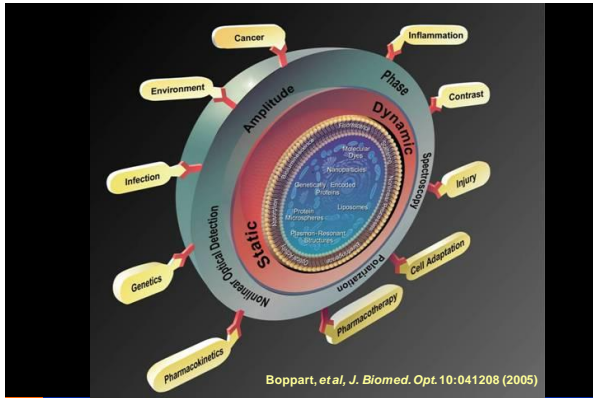



Halas group Nie group

Contrast in Imaging Modalities



- Magnetic Resonance
 - T₁ and T₂ differences
 - Gadolinium, SPIOs
- Nuclear Medicine
 - Radioactive isotopes
 - FDG in PET
- Optical Imaging
 - Bioluminescence
 - Fluorescence
 - Raman Shifts
 - Scattering / Absorption
- X-Ray Computed Tomography (CT)
 - Differential attenuation
 - Iodinated compounds
- Ultrasound
 - Acoustic impedance
 - Micro-bubbles



I Contrast Methods in OCT

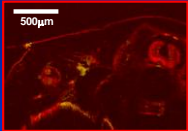
Functional (Physiological) OCT

- > Doppler (blood flow)
- > Standard deviation imaging & speckle contrast (movement)
- > Polarization-sensitive OCT (birefringence)

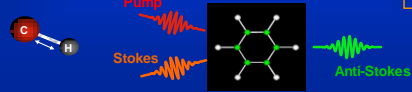
Endogenous Contrast in OCT

- > Spectroscopic OCT (melanin, Hb, HbO₂)
- > Second-harmonic generation OCT (collagen, ultrastructure)
- > Nonlinear interferometric vibrational imaging (molecular bonds)

Speckle contrast OCT image of a *Xenopus laevis* tadpole



Noise advantage to techniques with no background light



I Contrast Methods in OCT

Imaging Exogenous Probes

- > OCT does NOT sense fluorescence

Probe Engineering Issues

- > Synthesis methods
- > Size (scattering ↔ tissue transport)
- > Specificity of targeting
- > Biocompatibility

Detection Engineering Issues

- > Background discrimination (a priori information needed?)
- > Sensitivity

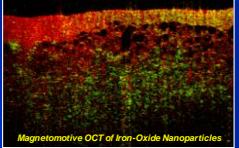
Synergistic Approach

Detection ↔ Synthesis

Adapt imaging methods for specific probes ↔ Adapt contrast agents for imaging

minimum detectable concentration < toxic concentration

Magnetoimotive OCT of Iron-Oxide Nanoparticles



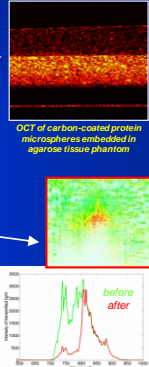
I Probe Detection Techniques in OCT

Exogenous Probe Detection Techniques

- > Scattering
 - Protein microspheres (Barton, *today*)
 - Plasmon-resonant nanoshells (Drezek)
- > Absorption
 - Plasmon-resonant nanocages (Xia)
 - Plasmon-resonant nanorods (*today*)
- > Spectroscopic absorption
 - NIR-absorbing dyes (*today*)
- > Transient absorption
 - methylene blue, ICG (Izatt)
- > Magnetomotive
 - magnetite nanoparticles (*today*)

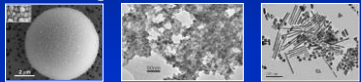
Require a priori information about sample

SOC image of a celery stalk with NIR dye in center (top). Laser spectrum before and after passage through absorbing dye (bottom).

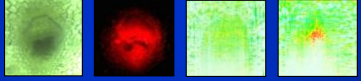


I OCT Molecular Contrast Enhancing Techniques

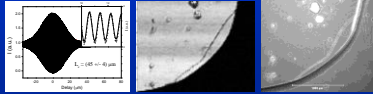
OCT Contrast Agents:



Spectroscopic OCT:



Nonlinear Interferometric Vibrational Imaging (NIVI):



Exogenous ↑

↓ Endogenous

OCT Contrast Agents: Overview

- Scattering agents**
protein microspheres*
liposomes
- Magnetic agents**
microsphere-encapsulated ferrofluids
nanoparticles* & ferrofluids
- Spectroscopic agents**
NIR absorbing dyes*
microsphere encapsulated dyes
carbon nanotubes
- Plasmon-resonant agents**
gold* nanorods

*FDA-type analogues

Protein Microsphere Structure

Iron-Oxide Nanoparticles

Protein Shell (BSA)

Surface

Oil Core (Vegetable Oil)

Synthesis of Protein Microspheres

Titanium Horn

Stainless Steel Collar

Gas Inlet /Outlet

Non Aqueous Liquid

5% WV Bovine Serum Albumin

Sphere size distribution via Coulter counter

Sonication power: 7 W
Sonication time: 3 min
Cell temp: 45-65 °C
Average size: 1.4 µm
Yield : 2.6 x 10⁸ microspheres/µL

Role of High-Intensity Ultrasound (20 KHz)
Formation of micro-emulsion
Chemical cross-linking with superoxide from water sonolysis
Control microsphere size (50 nm - 15 µm)

SEMs of iron-oxide nanoparticle colloid in core or in embedded monolayer in albumin microsphere shell

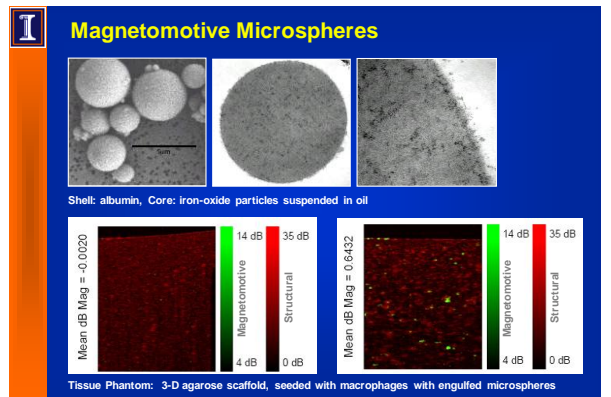
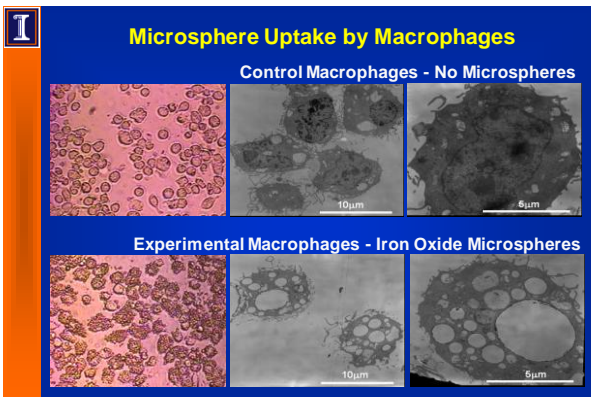
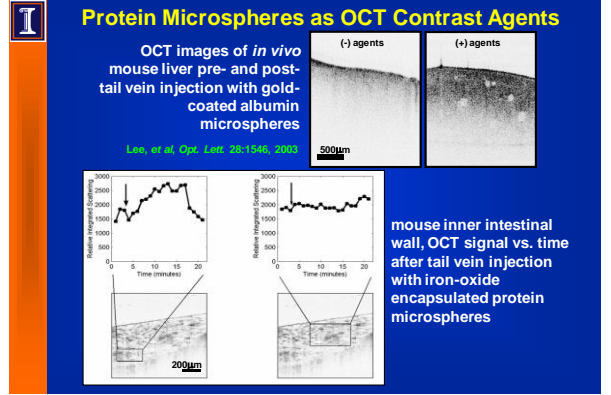
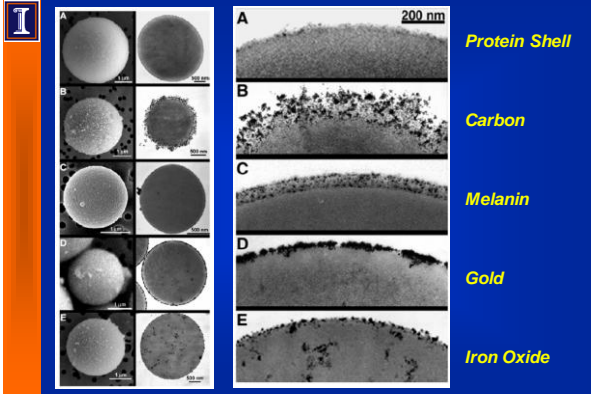
OCT Microsphere Contrast Agents

- Nanoparticles embedded in shell or encapsulated
- Synthesis via high-intensity ultrasound
- Diameters typically ~ 2µm
- Biocompatible

Shell: albumin, Core: iron-oxide particles suspended in oil

Engineered Microsphere Combinations

Protein Shells	Inner Cores	Surface Modifications
Albumin	Air, O ₂ , N ₂ , Ar	PEG
Hemoglobin	Vegetable oils	Fluorescein
Pepsin	Water	Iron oxide colloid
Immunoglobulins	Organic liquids	Immunoglobulins
Lipase	Acetoacetate	Folate
Peroxidases	Fluorocarbons	Gd complexes
Modified Myoglobin	Iodinated agents	Monoclonal Antibodies
	Gd complexes	Gold
	Ferrofluids	Carbon
		Melanin



I Integrin-Targeted Microspheres

RGD-Targeting of Integrin Receptors
 Hetero-dimeric trans-membrane receptor
 Cell attachment, survival, migration, proliferation, tumorigenesis, metastasis

Over 25 known integrin receptors
 Most recognize small tri-peptide RGD sequence (arginine-glycine-aspartic acid)

Integrins overexpressed in tumor cells, angiogenesis, atherosclerosis ($\alpha_v\beta_3$)

Fluorescence microscopy of RGD peptides and Nile Red microspheres
 HT29 Human Colon Tumor Cells

I In Vivo Integrin-Targeted Microspheres

MNU-rat model, RGD-Nile Red Microspheres

Cell lines **RGD coated microspheres** **Non-coated microspheres**

HUVEC	+++	+
SKBR-3	+ / -	-
Macrophages	+	+ / -
Empty cover slip	+	+ / -

I Background-Free Contrast Agent Imaging

Magnetically-susceptible agents:

- Human tissue not ferromagnetic
- Displacement or rotation induced by B
- Modulate optical scattering
- B switched on & off with successive depth scans – difference image

M-mode of magnetite particle in agarose with modulated B-field

transverse displacement axial displacement rotation of anisotropic agent

I Motivation: Targeted Imaging Contrast in OCT

Contrast agents figures of merit:

- NIR scattering or absorption
- Background discrimination
- Biocompatibility
- Size < 200 nm
- Molecular specificity

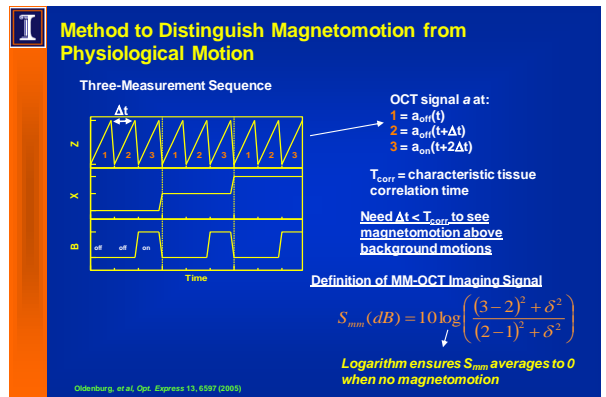
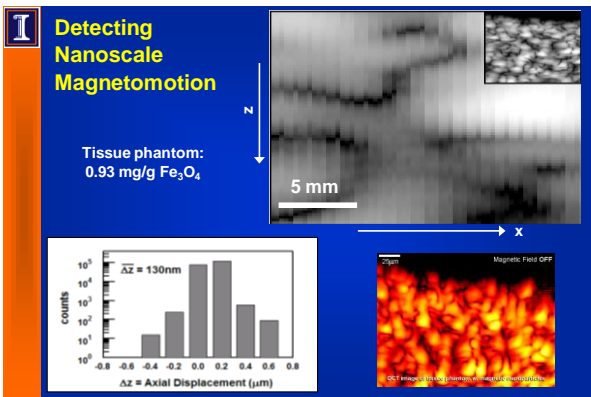
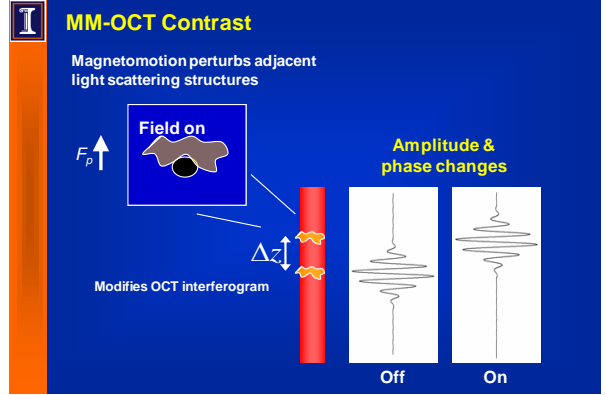
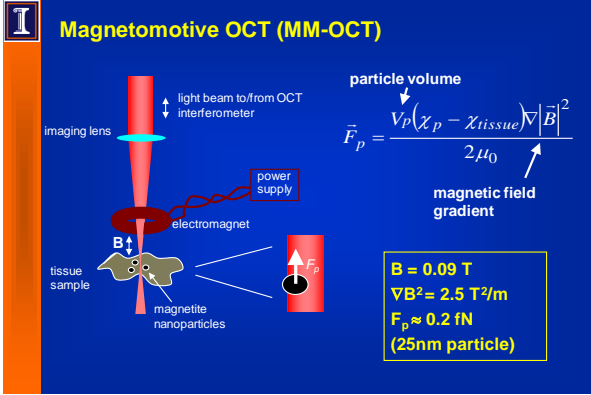
Magnetic Contrast Agents

- Externally controllable!
- High magnetic susceptibility χ
- Overlap with MRI contrast agent technology

$\frac{\chi_{Fe_3O_4} - 1}{|\chi_{tissue}|} < 10^{-5} \Rightarrow$ Contrast of up to $10^5!$

Ocean Nanotech Sigma-Aldrich

Carboxyl-terminated magnetite (Fe_3O_4) nanoparticles



Tissue Phantoms

Optically & mechanically simulate tissue

OCT images

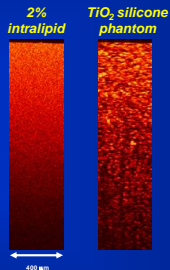
Optical: TiO₂ microparticles 4 mg/g (≈ 2% Intralipid)

Mechanical: silicone matrix w/ tailored elasticity (10:1 PDMS + GE-RTV 615)

Magnetic: Fe₃O₄ nanoparticles 20-30 nm (Sigma-Aldrich #310069)

Answer questions:

- Dependence of MM-OCT signal on:
 - magnetic field strength B
 - magnetic particle concentration
 - optical scattering
- Sensitivity of MM-OCT



Predicted Scaling of MM-OCT

Force induced by magnetic field:

$$\vec{F}_p = V_p (\vec{M} \cdot \nabla) \vec{B} \propto \nabla |\vec{B}|^2 \text{ (low field)}$$

$$\propto \nabla |\vec{B}| \text{ (saturated)}$$

Displacement in elastic medium:

$$\Delta z \propto \frac{\rho F_p}{E}$$

← Elastic modulus

OCT signal change caused by displacement:

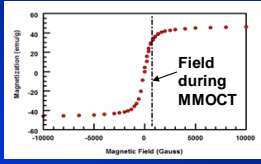
$$\Delta a_{mm} \propto s |\Delta z|$$

↑ Speckle-averaged scattering

Predicted Scaling Law:

$$\Delta a_{mm} \propto s^{n_s=1} \rho^{n_\rho=1} B^{n_B=1.0 \text{ or } 2}$$

SQUID magnetometry



Detection sensitivity - 220 ppm (Theoretical - 2 ppm)

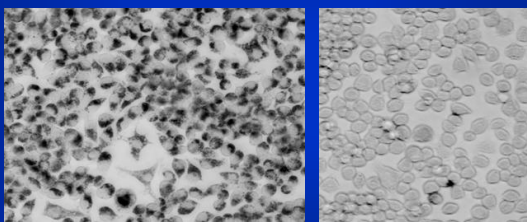
Oldenburg, et al., Opt. Express 13, 6597 (2005)

Magnetomotive OCT in Practice

Macrophages (J774A.1)

Ocean Nanotech
20 nm magnetite, 0.15 mg/mL overnight exposure

Control



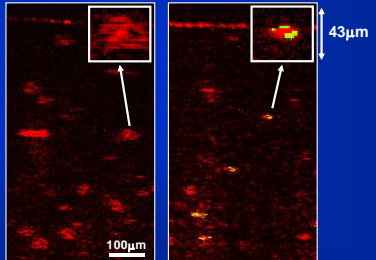
Trypan blue → no loss of viability (> 99%)

Cell Labeling with Magnetic Optical Contrast Agents

Macrophages (J774A.1) in three-dimensional agarose gel scaffold

Control cells

Cells with ~50% uptake of magnetite



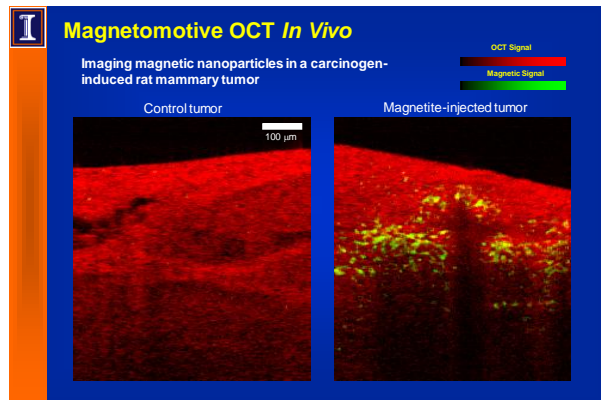
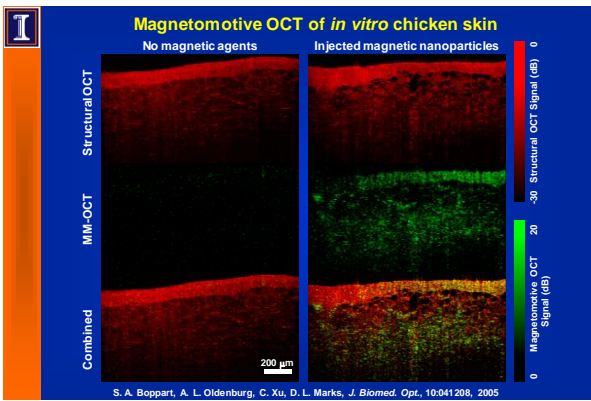
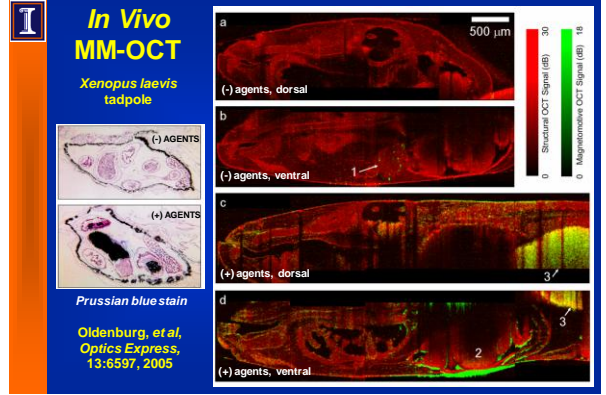
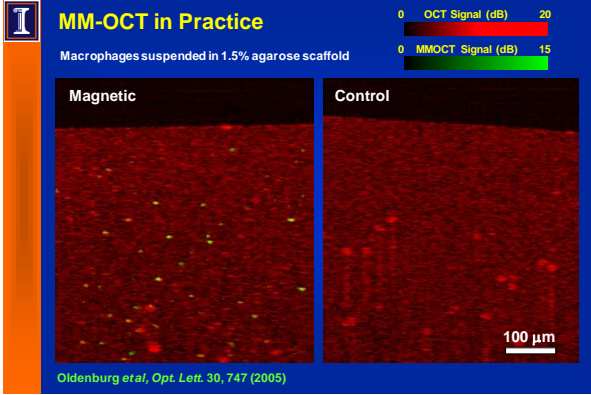
Structure
Magnetic

microscopy of magnetite-exposed macrophages in scaffold

100 μm

43 μm

Oldenburg, et al., Optics Letters, 30:747, 2005



Magnetomotive OCT *In Vivo*

Delivery via tail-vein injection

Control Injected

Structural OCT Magnetomotive OCT

Nanoparticle Injected

Structural OCT Magnetomotive OCT

200 μm

Rat spleen distribution of magnetic nanoparticles euthanized 2 hours after tail vein injection.

Magnetomotive Optical Coherence Elastography

- Optical and mechanical properties of phantom similar to those of tissue
- Magnetic nanoparticles homogeneously dispersed in sample volume

Optical scatterers:
TiO₂ microparticles 4 mg/g (avg. size 1 μm)

Mechanical simulator:
silicone matrix with tailored elasticity (10:1 PDMS + GE-RTV 615)

Magnetic agents:
Fe₃O₄ nanoparticles 20-30 nm (Sigma-Aldrich #310069); mass concentration 2.5 mg/g

MM-OCE Transients

- $f_{\text{Bmod}} = 6.67 \text{ Hz}$; duty cycle = 33%
- Camera line rate = 1 kHz, M-mode imaging

A-scan amplitude

100 μm

M-mode imaging $\rightarrow a(t), x(t)$

vertical scale bar = 0.3 mm

Magnetomotive Optical Coherence Elastography

- evidence of underdamped oscillations in sample when magnetic impulse exerted:

A-scan amplitude

100 μm

M-mode imaging $\rightarrow a(t), x(t)$

$y(t) = Ae^{-\gamma t} \cos(\omega t - \delta) + C$

- damping coefficient \leftrightarrow viscosity
- oscillation frequency \leftrightarrow elasticity

$\gamma = 82.86 \text{ s}^{-1}$

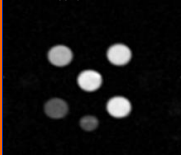
$\omega = 450.9 \text{ rad/s} \Rightarrow f = \frac{\omega}{2\pi} = 72 \text{ Hz}$

Magnetic Nanoparticle MRI Contrast

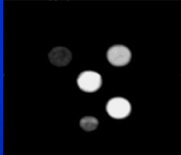
Negative T_2 contrast due to particle magnetization
 → same figure of merit as in MM-OCT!

MRI of agarose phantoms dosed with Ocean Nanotech 20 nm magnetite

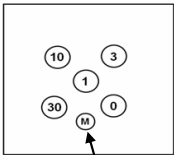
$T_{echo} = 11\text{ ms}$



$T_{echo} = 50\text{ ms}$



Dose in ppm



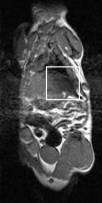
Marker

Spin-echo MRI, 4.7T Sisco, $T_{repetition} = 4s$
 Collaboration with B. Odintsov, Beckman Imaging Center

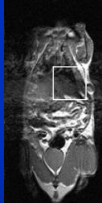
In Vivo Magnetic Nanoparticle MRI Contrast

MNU rat mammary tumor model, non-targeted agents
 Negative T_2 contrast due to particle magnetization

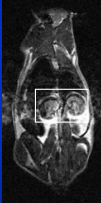
(-) agents



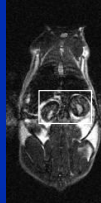
(+) agents



(-) agents



(+) agents



Spin-echo MRI, 4.7T Sisco, $T_{repetition} = 4s$
 Collaboration with B. Odintsov, Beckman Imaging Center

Protein Microspheres as an MM-OCT Contrast Agent

5% Agarose Gel

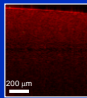
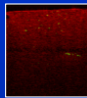
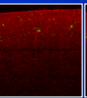
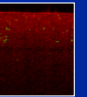
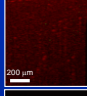
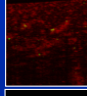
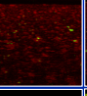
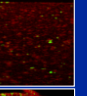
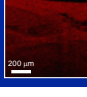
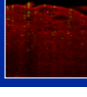
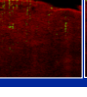
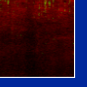
- (-) 0.074 dB (n = 11)
- (+) 1.130 dB (n = 11)

Macrophage Uptake


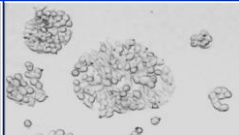
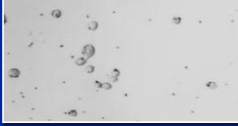
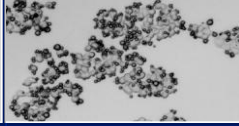
- (-) 0.018 dB (n = 11)
- (+) 0.411 dB (n = 11)

In Vivo Intra-Tumor Injection

- (-) 0.002 dB (n = 21)
- (+) 0.598 dB (n = 21)

	(-) Microspheres	(+) Microspheres		
5% Agarose Gel				
Macrophage Uptake				
In Vivo Intra-Tumor Injection				

Cell Studies Targeting Specificity

	CRL - 4010 ($\alpha_v\beta_3$) Human Mammary Epithelium	HT - 29 ($\alpha_v\beta_3$) Human Colon Adenocarcinoma
Non-Targeted		
RGD-Targeted		

Animal Studies (Atherosclerosis)

- Control Rat: Normal Diet
- MM-OCT Results: Mean dB Mag = 0.027 dB (n=17)

Animal Studies (Atherosclerosis)

- Atherosclerotic Rat
 - High Fat, High Cholesterol Diet
 - Euthanized at 10 Weeks on Diet
- MM-OCT Results:
 - Mean dB Mag - All Images = 0.329 dB (n=17)
 - Mean dB Mag - Images with Focal Magnetic Signal = 0.931 dB (n=5)
 - Mean dB Mag - Images with no MM Signal = 0.077 dB (n=12)

Animal Studies (Atherosclerosis)

MM-OCT
Mag dB = 2.218 dB

H&E Histology

Spectroscopic OCT

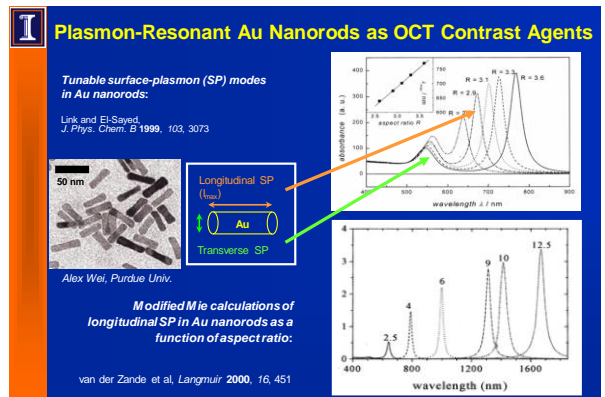
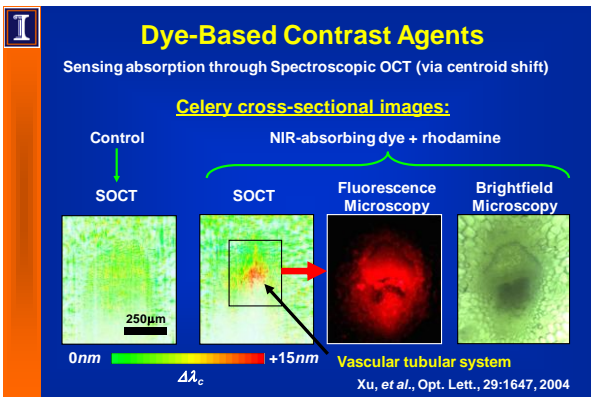
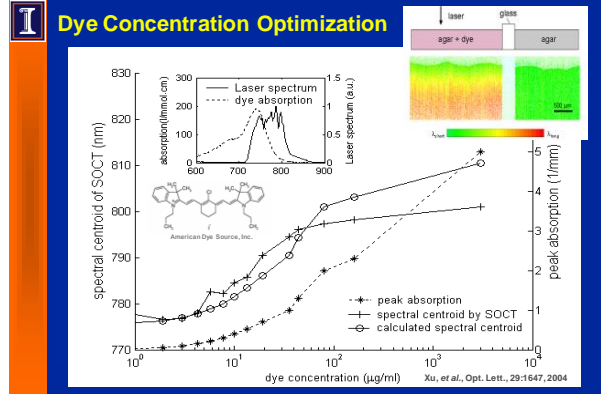
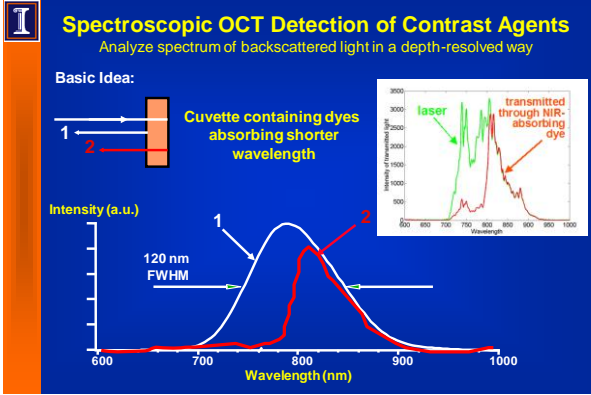
Envelope: Structural OCT

- ⇒ Amplitude Reflection
- ⇒ Reflectivity / Scattering

Carrier: Spectroscopic OCT

- ⇒ Spectral Reflection
- ⇒ Scattering / Absorption

Traditionally performed in TD-OCT, and SD-OCT offers phase stability



Magnetic Plasmon-Resonant Gold Nanorods

Extinction Spectrum of GNRs

Tri-saph Laser Spectrum

Synthesis of IONP-GNR Hybrids Using EDC/Sulfo-NHS (APL1-142)

Magnetic Gold Nanorods

TEM

Oldenburger, et al., J Mat Chem, 2009

H & E Histology

Two-Photon Luminescence

TEM

Asymmetric Single-Walled Carbon Nanotube/iron Oxide Nanoparticle Complexes

Figure 3. (a) TEM image of asymmetric SWCNTs synthesized with Fe-Functionalized SWCNTs. (b) TEM image of asymmetric SWCNTs synthesized with Fe-Functionalized SWCNTs. (c) TEM image of asymmetric SWCNTs synthesized with Fe-Functionalized SWCNTs. (d) TEM image of asymmetric SWCNTs synthesized with Fe-Functionalized SWCNTs. (e) TEM image of asymmetric SWCNTs synthesized with Fe-Functionalized SWCNTs. (f) TEM image of asymmetric SWCNTs synthesized with Fe-Functionalized SWCNTs. (g) TEM image of asymmetric SWCNTs synthesized with Fe-Functionalized SWCNTs. (h) TEM image of asymmetric SWCNTs synthesized with Fe-Functionalized SWCNTs. (i) TEM image of asymmetric SWCNTs synthesized with Fe-Functionalized SWCNTs. (j) TEM image of asymmetric SWCNTs synthesized with Fe-Functionalized SWCNTs. (k) TEM image of asymmetric SWCNTs synthesized with Fe-Functionalized SWCNTs. (l) TEM image of asymmetric SWCNTs synthesized with Fe-Functionalized SWCNTs. (m) TEM image of asymmetric SWCNTs synthesized with Fe-Functionalized SWCNTs. (n) TEM image of asymmetric SWCNTs synthesized with Fe-Functionalized SWCNTs. (o) TEM image of asymmetric SWCNTs synthesized with Fe-Functionalized SWCNTs. (p) TEM image of asymmetric SWCNTs synthesized with Fe-Functionalized SWCNTs. (q) TEM image of asymmetric SWCNTs synthesized with Fe-Functionalized SWCNTs. (r) TEM image of asymmetric SWCNTs synthesized with Fe-Functionalized SWCNTs. (s) TEM image of asymmetric SWCNTs synthesized with Fe-Functionalized SWCNTs. (t) TEM image of asymmetric SWCNTs synthesized with Fe-Functionalized SWCNTs. (u) TEM image of asymmetric SWCNTs synthesized with Fe-Functionalized SWCNTs. (v) TEM image of asymmetric SWCNTs synthesized with Fe-Functionalized SWCNTs. (w) TEM image of asymmetric SWCNTs synthesized with Fe-Functionalized SWCNTs. (x) TEM image of asymmetric SWCNTs synthesized with Fe-Functionalized SWCNTs. (y) TEM image of asymmetric SWCNTs synthesized with Fe-Functionalized SWCNTs. (z) TEM image of asymmetric SWCNTs synthesized with Fe-Functionalized SWCNTs.

Figure 4. (a) Raman spectra of asymmetric SWCNTs synthesized with Fe-Functionalized SWCNTs. (b) Raman spectra of asymmetric SWCNTs synthesized with Fe-Functionalized SWCNTs. (c) Raman spectra of asymmetric SWCNTs synthesized with Fe-Functionalized SWCNTs. (d) Raman spectra of asymmetric SWCNTs synthesized with Fe-Functionalized SWCNTs. (e) Raman spectra of asymmetric SWCNTs synthesized with Fe-Functionalized SWCNTs. (f) Raman spectra of asymmetric SWCNTs synthesized with Fe-Functionalized SWCNTs. (g) Raman spectra of asymmetric SWCNTs synthesized with Fe-Functionalized SWCNTs. (h) Raman spectra of asymmetric SWCNTs synthesized with Fe-Functionalized SWCNTs. (i) Raman spectra of asymmetric SWCNTs synthesized with Fe-Functionalized SWCNTs. (j) Raman spectra of asymmetric SWCNTs synthesized with Fe-Functionalized SWCNTs. (k) Raman spectra of asymmetric SWCNTs synthesized with Fe-Functionalized SWCNTs. (l) Raman spectra of asymmetric SWCNTs synthesized with Fe-Functionalized SWCNTs. (m) Raman spectra of asymmetric SWCNTs synthesized with Fe-Functionalized SWCNTs. (n) Raman spectra of asymmetric SWCNTs synthesized with Fe-Functionalized SWCNTs. (o) Raman spectra of asymmetric SWCNTs synthesized with Fe-Functionalized SWCNTs. (p) Raman spectra of asymmetric SWCNTs synthesized with Fe-Functionalized SWCNTs. (q) Raman spectra of asymmetric SWCNTs synthesized with Fe-Functionalized SWCNTs. (r) Raman spectra of asymmetric SWCNTs synthesized with Fe-Functionalized SWCNTs. (s) Raman spectra of asymmetric SWCNTs synthesized with Fe-Functionalized SWCNTs. (t) Raman spectra of asymmetric SWCNTs synthesized with Fe-Functionalized SWCNTs. (u) Raman spectra of asymmetric SWCNTs synthesized with Fe-Functionalized SWCNTs. (v) Raman spectra of asymmetric SWCNTs synthesized with Fe-Functionalized SWCNTs. (w) Raman spectra of asymmetric SWCNTs synthesized with Fe-Functionalized SWCNTs. (x) Raman spectra of asymmetric SWCNTs synthesized with Fe-Functionalized SWCNTs. (y) Raman spectra of asymmetric SWCNTs synthesized with Fe-Functionalized SWCNTs. (z) Raman spectra of asymmetric SWCNTs synthesized with Fe-Functionalized SWCNTs.

Choi, et al., Nanoletters, 7:861-867, 2007

Summary and Conclusions

- Optical scattering-based images (OCT) frequently exhibit poor inherent contrast
- Novel scattering, absorbing, and modulating contrast enhancing techniques have the potential to improve the diagnostic ability of these imaging techniques
- Significant potential for therapeutic applications
- **Exogenous Contrast Agents**
 - Scattering microspheres & liposomes
 - Magnetically-modulated agents
 - Absorbing chemical dyes
 - Plasmon-resonant nanorods
- **Endogenous Spectroscopic Detection**
 - Spectroscopic OCT (Absorption & Scattering)
 - Nonlinear Interferometric Vibrational Imaging (NIVI)
 - CARS, SHG, THG

Outline

Lecture 1 (today)

- Optical Coherence Tomography (OCT)
- Beam Delivery Instruments
- Morphological & Cellular OCT Imaging
- Spectroscopic OCT
- Application to Cancer Imaging

Lecture 2 (next week)

- Molecular OCT Imaging
- Contrast Agents for OCT
 - Scattering, Absorbing, Modulating Probes




Acknowledgments


Beckman Institute
Biophotonics Imaging Laboratory
Stephen Boppart, M.D., Ph.D.



<p>Graduate Students</p> <p>Adeel Ahmad Wladimir Benalcazar Vasilica Crecea, M.S. Budiman Dabarsyah, M.S. Ben Graf Di Li</p> <p>Research Specialists Eric Chaney, Darold Spillman</p> <p>Medical Oncology: Surgical Oncology: Pathology: Otolaryngology:</p>	<p>Graduate Students</p> <p>Yuan Liu, M.S. Leon Liang, M.S. Cac Nguyen Freddy Nguyen Sunghwan Shin</p> <p>Clinical Collaborators: Kendriith Rowland, M.D. Jan Kotynek, M.D. George Liu, M.D. John Brockenbrough, M.D.</p>	<p>Research Scientists</p> <p>Steven Adie, Ph.D. Joe Geddes, Ph.D. Zhi Jiang, Ph.D. Renu John, Ph.D. Woonggyu Jung, Ph.D. Marina Marjanovic, Ph.D. Utkarsh Sharma, Ph.D. Haohua Tu, Ph.D.</p> <p>Patricia Johnson, M.D., Ph.D. Uretz Oliphant, M.D. Krishnan Tangella, M.D. Michael Novak, M.D.</p>
---	---	--

National Institutes of Health (Roadmap, NIBIB, NCI), National Science Foundation, Grainger Foundation, Carle Foundation Hospital

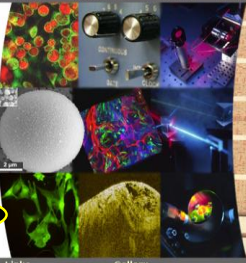
BIOPHOTONICS IMAGING LABORATORY



Home
Technology
Research
Publications
Presentations
Academics
Prof. Boppart
News


Located in the Beckman Institute for Advanced Science and Technology at the University of Illinois at Urbana-Champaign, the Biophotonics Imaging Laboratory, directed by Professor Stephen Boppart, is dedicated to the development of optical biomedical imaging techniques.

Optical coherence tomography (OCT) is the core technology used within the lab. OCT is promising for the early detection and diagnosis of various pathologies and can also be used in many types of biological research.



biophotonics.illinois.edu

Personnel
Links
Gallery
Facilities


Beckman Institute
For advanced science and technology
